Effect of CO_2 laser cutting process parameters on edge quality and operating cost of AISI316L

H. A. Eltawahni[1], M. Hagino[2], K. Y. Benyounis[1], T. Inoue[2] and A. G. Olabi[3]

1. Industrial Eng. Dept., Benghazi University, P. O. Box 1308, Benghazi- Libya hayat.eltawahni2@mail.dcu.ie, Khaled.benyounis2@mail.dcu.ie.
2. Department of Mechanical Engineering, Daido University, 10-3, Takiharu-cho, Minami-ku, Nagoya, Japan, Postcode 457-8530, mas.hagino@gmail.com and takinoue@daido-it.ac.jp
3. School of Mech. & Manu. Eng., Dublin City University, Dublin 9, Ireland, Abdul.olabi@dcu.ie.

ABSTRACT

Laser cutting is a popular manufacturing process utilized to cut various types of materials economically. The width of laser cut or kerf, quality of the cut edges and the operating cost are affected by laser power, cutting speed, assist gas pressure, nozzle diameter and focus point position as well as the work-piece material. In this paper CO_2 laser cutting of stainless steel of medical grade AISI316L has been investigated. Design of experiment (DOE) was implemented by applying Box-Behnken design to develop the experiment lay-out. The aim of this work is to relate the cutting edge quality parameters namely: upper kerf, lower kerf, the ratio between them, cut section roughness and operating cost to the process parameters mentioned above. Then, an overall optimization routine was applied to find out the optimal cutting setting that would enhance the quality or minimize the operating cost. Mathematical models were developed to determine the relationship between the process parameters and the edge quality features. Also, process parameters effects on the quality features have been defined. Finally, the optimal laser cutting conditions have been found at which the highest quality or minimum cost can be achieved.

KEYWORDS: CO_2 laser cutting, AISI316L, optimization.

1- INTRODUCTION

Laser beam cutting (LBC) process has a wide range of applications in different manufacturing processes in industry due to its advantages of high cut quality and cost effectiveness through mass-production rate [1]. The material to be cut is locally melted by the focused laser beam. The melt is then blown away with the aid of assist gas, which flow coaxially with the laser beam, forming a kerf. In metal cutting procedures, different types of assist gases

are used such as oxygen and nitrogen. The selection of an appropriate gas type or a mixture of gases with a given mixing percentage is fundamental to minimize the cutting cost by increasing the cutting speed [1-2]. Changing the assist gas composition and its effect on laser cutting of 3 mm mild steel has been studied by Chen [3]. The gas mixtures used were composed of oxygen, argon, nitrogen and helium. He reported that using oxygen with high purity along with laser power of 1500 W is required for high performance laser cutting for this material. Ghany and Newishy [4] have investigated the effect of pulsed and continuous wave (CW) Nd-YAG laser cutting of austenitic stainless steel sheets using nitrogen or oxygen as an assist gas. It was shown that the laser cutting quality depends mainly on the laser power, pulse frequency, cutting speed and focus position. Compared to oxygen, nitrogen produced a brighter and smoother cut surface with smaller kerf, although it did not prove to be economical. The effect of varying the process input parameters on the quality characteristics such as kerf width and its variation along the cut was the interest of many studies. Chen [5] has investigated CO_2 laser cutting of 3 mm-thick mild steel sheet. It was reported that as the laser power increases and cutting speed decreases the kerf width increases. He also observed that oxygen or air leads to wider kerf, however, a narrow kerf could be obtained by using inert gas as an assist gas. The same variation in the kerf width with cutting speed, laser power, and type of gas and pressure has been found by Ghany and Newishy in their experiment [4]. Uslan [6] has found that increasing the laser power intensity enhances the kerf width size and this is more pronounced with reducing cutting speed. It was reported that a small variation in laser power results in a large variation in the kerf size. He reported that the influence of cutting speed less than that corresponding to the laser power. Also, he mentioned that by using defocused laser beam, which in retrain reduces the laser power density, would increase the kerf width size. Yilbas [7] has mentioned that increasing laser power and energy coupling factor increase the kerf width size. Also, he reported that any increase in the cutting speed reduces the kerf width. It was found that the laser power has a highly significant effect on the kerf size. Yilbas [8] reported that increasing laser beam scanning speed reduces the kerf width, while the kerf width increases with increasing laser power. It was reported that the main effects of all the parameters employed have a significant influence on the cut quality. Dilthey et al. [9] have mentioned that when cutting stainless steel, exact adjustment of focus position and gas jet is essential in order to obtain dross free cutting. Also, they reported that the corrosion resistance is at risk when cutting stainless steel with oxygen but the cutting speed is high or vice

versa when cutting stainless steel using inert gas. Yilbas and Rashid [10] have monitored the dross ejection from the kerf, the frequency of the dross ejection correlated with the striation frequency and out of flatness. It was mentioned that the cutting speed and thickness have a significant effect on the out of flatness. They indicated that the cut quality can be improved by varying the combination of pulse frequency and output intensity. Radovanovic and Dasic [11] have observed that the surface roughness increases along with the sheet thickness, but decreases with increasing the laser power when cutting mild steel. Neimeyer et al. [12] have indicated that the average surface roughness may be best at high cutting speed and low assist gas pressure. They confirmed that the workpiece thickness showed little effect on the cut surface quality. It was concluded that the profiles of the cut surface of the top and bottom edges yield the same values for average surface roughness, despite the significant visual difference in the striation pattern.

In order to obtain the desirable high level of cutting edge quality it is important to choose the optimal combinations of the process parameters as these parameters have an effect on the output characteristics or quality features namely: upper kerf, lower kerf and cutting edge roughness etc. In this case, a systematic study based on Design of experiment (DOE) is required to find out the functional relationship between the output characteristics and the process input parameters with the minimum number of experiments. Several investigations were performed using systematic approaches to optimize the LBC process. Dubey and Yadava [13] have applied Taguchi method and RSM to optimize the LBC process of thin sheet of high silicon-alloy steel, taking into account multi-performance characteristics. Also, the same authors [14] have applied Taguchi method to investigate the effect of LBC process parameters on the kerf width, kerf deviation and kerf taper when cutting nickel-based super-alloy sheets. Their aim was to optimize the process. Yilbas [15] has reported the effect of cutting parameters on kerf size variations of thick sheet metals. He proposed a factorial analysis to identify the main effects and interactions of the parameters. It is found that laser output power and oxygen gas pressure have significant effect on the percentage of kerf width variation. Eltawahni et al. [16, 17 and 18] have applied RSM to investigated and optimize the LBC of ultrahigh molecular weight polyethylene, medium density fibreboard and Polymethyl-methacrylate. They concluded that the higher cutting speed does not always improve the efficiency of the LBC. Finally they presented the optimal cutting conditions for both economical and high quality cut. Other researchers have highlighted the importance of modelling and optimizing the laser cutting process for different materials [19-21].

Thus, the aim of this paper is to apply RSM to develop mathematical models to predict the width of upper kerf, lower kerf, the ratio between the upper and lower kerfs, cut section roughness and operating cost for CW CO_2 laser cutting of AISI316 austenitic stainless steel. The second aim is to use the developed models to optimize the cutting operation. The laser cutting input parameters taken into consideration are laser power (A), cutting speed (B), focal point position (C), gas pressure (D) and nozzle diameter (E).

2. EXPERIMENTAL DESIGN

The experiment was designed based on a three level Box-Behnken design with full replication [22 and 23]. Laser power (1 - 1.5 kW), cutting speed (1000 - 3000 mm/min), focal point position (-4 to -2 mm), nitrogen pressure (10 – 15 bar) and nozzle diameter (1, 1.5 and 2 mm) are the process input parameters. Table 1 shows LBC parameters and experimental design levels used. RSM was applied to the experimental data using statistical software, Design-Expert V7. Second order polynomials were fitted to the experimental data to obtain the regression equations. The sequential F-test, lack-of-fit test and other adequacy measures were used to select the best fit. A step-wise regression method was used to fit the second order polynomial Eq. 1 to the experimental data and to find the significant model terms [23, 24]. The same statistical software was used to generate the statistical and response plots as well as the optimization.

$$Y = b_o + \sum b_i \chi_i + \sum b_{ii} \chi_{ii}^2 + \sum b_{ij} \chi_i \chi_j \qquad (1)$$

Table 1: Process variables and experimental design levels used.

Parameter	Code	Unit	-1	0	+1
Laser power	A	kW	1	1.25	1.5
Cutting speed	B	mm/min	1000	2000	3000
Focal point position	C	mm	-4	-3	-2
Nitrogen pressure	D	Bar	10	12.5	15
Nozzle diameter*	E	mm	1	1.5	2

* Categorical factor.

3. EXPERIMENTAL WORK

3.1 Laser Cutting

Austenitic stainless steel in sheet form of standard grade of AISI316L was used as workpiece material. The sheet dimensions were 500 x 500 mm with thickness of 2 mm. Trial runs of laser cutting were performed by varying one of the process factors at-a-time to determine the range of each factor. Full cut, keeping the kerf width, cutting edge striations and dross to a minimum; were the criteria of selecting the working ranges. The main experiment was performed according to the design matrix in a random order to avoid any systematic error. A CW 1.5 kW CO_2 Rofin laser provided by Mechtronic Industries Ltd and a focusing lens with focal length of 127 mm were used to perform the cut. Nitrogen gas was supplied coaxially as an assist gas with different pressures. Specimens were cut from the plate for each condition. The specimen shape was designed in order to allow the measurement of the responses in a precise and easy way. The upper and lower kerf widths were measured using an optical microscope which has an accuracy of 0.001 and allows measurements in both the x-axis and y-axis directions. The average of five measurements of both kerf widths was recorded for all runs. The ratio of the upper kerf to the lower kerf was calculated for each run using the averaged data. The arithmetic average roughness parameter, R_a, values were measured using a surface roughness tester model TR-200. Five consistent surface roughness values of each specimen were measured at the centre of the cut surface and an average was calculated for each specimen. The design matrix and the average measured responses are shown in Table 2 and 3.

Table 2: Design matrix.

Factors						
Std	**Run**	**A, kW**	**B, mm/min**	**C, mm**	**D, Bar**	**E, mm**
1	21	1	1000	-3	12.5	1.5
2	33	1.5	1000	-3	12.5	1.5
3	41	1	3000	-3	12.5	1.5
4	45	1.5	3000	-3	12.5	1.5
5	40	1.25	2000	-4	10	1.5
6	23	1.25	2000	-2	10	1.5
7	5	1.25	2000	-4	15	1.5
8	25	1.25	2000	-2	15	1.5
9	2	1.25	1000	-3	12.5	1
10	34	1.25	3000	-3	12.5	1
11	1	1.25	1000	-3	12.5	2
12	19	1.25	3000	-3	12.5	2
13	17	1	2000	-4	12.5	1.5
14	24	1.5	2000	-4	12.5	1.5
15	18	1	2000	-2	12.5	1.5
16	8	1.5	2000	-2	12.5	1.5
17	7	1.25	2000	-3	10	1
18	6	1.25	2000	-3	15	1
19	15	1.25	2000	-3	10	2
20	12	1.25	2000	-3	15	2
21	39	1.25	1000	-4	12.5	1.5
22	30	1.25	3000	-4	12.5	1.5
23	20	1.25	1000	-2	12.5	1.5
24	36	1.25	3000	-2	12.5	1.5
25	3	1	2000	-3	10	1.5
26	46	1.5	2000	-3	10	1.5
27	4	1	2000	-3	15	1.5
28	28	1.5	2000	-3	15	1.5
29	38	1.25	2000	-4	12.5	1
30	29	1.25	2000	-2	12.5	1
31	27	1.25	2000	-4	12.5	2
32	11	1.25	2000	-2	12.5	2
33	13	1	2000	-3	12.5	1
34	16	1.5	2000	-3	12.5	1
35	37	1	2000	-3	12.5	2
36	42	1.5	2000	-3	12.5	2
37	10	1.25	1000	-3	10	1.5
38	9	1.25	3000	-3	10	1.5
39	14	1.25	1000	-3	15	1.5
40	26	1.25	3000	-3	15	1.5
41	43	1.25	2000	-3	12.5	1.5
42	35	1.25	2000	-3	12.5	1.5
43	32	1.25	2000	-3	12.5	1.5
44	22	1.25	2000	-3	12.5	1.5
45	31	1.25	2000	-3	12.5	1.5
46	44	1.25	2000	-3	12.5	1.5

Table 3: Average of experimentally measured responses for AISI316L.

No.	upper kerf, mm	Lower kerf, mm	Ratio	Ra, μm	Operating cost, €/m
1	0.296	0.203	1.461	0.792	2.8921
2	0.325	0.227	1.435	0.732	2.9056
3	0.222	0.147	1.512	1.648	0.9640
4	0.241	0.216	1.119	0.804	0.9685
5	0.263	0.183	1.435	1.735	1.1890
6	0.221	0.224	0.988	0.394	1.1890
7	0.293	0.218	1.348	2.161	1.7099
8	0.265	0.157	1.688	0.693	1.7099
9	0.300	0.233	1.288	0.967	1.3360
10	0.194	0.145	1.341	0.734	0.4453
11	0.321	0.191	1.685	0.870	5.0868
12	0.223	0.167	1.337	0.814	1.6956
13	0.264	0.184	1.430	1.633	1.4461
14	0.307	0.212	1.450	0.910	1.4528
15	0.196	0.206	0.952	0.665	1.4461
16	0.231	0.245	0.940	0.409	1.4528
17	0.196	0.147	1.333	0.556	0.5522
18	0.264	0.209	1.265	0.610	0.7838
19	0.254	0.171	1.488	0.633	2.0803
20	0.289	0.190	1.521	0.490	3.0065
21	0.321	0.246	1.304	0.733	2.8988
22	0.250	0.182	1.371	1.039	0.9663
23	0.309	0.258	1.199	0.781	2.8988
24	0.180	0.173	1.042	0.578	0.9663
25	0.197	0.162	1.216	1.033	1.1856
26	0.235	0.188	1.246	0.481	1.1923
27	0.251	0.155	1.625	0.835	1.7065
28	0.314	0.192	1.634	0.449	1.7133
29	0.268	0.182	1.470	0.942	0.6680
30	0.242	0.216	1.122	0.620	0.6680
31	0.305	0.200	1.523	0.582	2.5434
32	0.263	0.230	1.145	0.744	2.5434
33	0.237	0.171	1.384	0.755	0.6646
34	0.281	0.186	1.511	0.634	0.6714
35	0.272	0.197	1.377	0.697	2.5400
36	0.303	0.186	1.630	0.522	2.5468
37	0.315	0.180	1.750	1.211	2.3779
38	0.211	0.174	1.213	0.743	0.7926
39	0.350	0.246	1.419	0.883	3.4198
40	0.264	0.159	1.659	0.479	1.1399
41	0.325	0.168	1.935	0.757	1.4494
42	0.312	0.167	1.863	0.613	1.4494
43	0.289	0.161	1.797	0.561	1.4494
44	0.301	0.174	1.735	0.694	1.4494
45	0.302	0.171	1.763	0.601	1.4494
46	0.297	0.193	1.539	0.683	1.4494

3.2 Estimating the Operating Cost

Laser cutting operating costs can be estimated as cutting per hour or per unit length. The laser system used in this work utilized CO_2 using a static volume of laser gases of approximately 7.5 litre every 72 hours. For this laser system with 1.5 kW maximum outputs power the operating costs generally falls into the categories listed in Table 4. The operating cost calculation does not account for any unscheduled breakdown and maintenance, such as a breakdown in the table motion controller or PC hard disc replacement [17]. The total approximated operating cost per hour as a function of process parameters can be estimated by $2.654+1.376xP + 9.60x10^{-3}xF$. However, the total approximated operating cost per unit length of the cut is given by Eq. 1, assuming 85% utilization. Eq. 2 was used to calculate the cutting cost per meter for all samples.

Table 4: Operating costs break down when nitrogen is used.

Element of cost	**Calculations**	**Cutting cost €/hr**
Laser electrical power	(20.88 kVA)(0.8 pf)(€0.12359/kWhr) x(P/1.5)	1.376xP
Chiller electrical power	(11.52 kVA)(0.8 pf)(€ 0.12359/kWhr)	1.139
Motion controller power	(4.8 kVA)(0.8 pf)(€ 0.12359/kWhr)	0.475
Exhaust system power	(0.9 kWhr)(€ 0.12359/kWhr)	0.111
Laser gas LASPUR208	{(€1043.93/ bottle)/(1500litre/bottle)}x 7.5 litre/72hr	0.072
Gas bottle rental	(€181.37/720hr)	0.252
Chiller additives	(€284.80/year)/(8760 hr/year)	0.033
Compressed nitrogen	€9.60 x 10^{-3}/litre x F[litre/hr]	$9.60x10^{-3}xF$
Nozzle tip	(€7.20/200hr)	0.036
Exhaust system filters	(€5/100hr)	0.05
Focus lens	(€186/lens)/(1000hr)	0.186
Maintenance labour (with overhead)	(12 hr/2000hrs operation)(€50/hr)	0.30
Total operation cost per hour		$2.654+1.376xP +9.60 x10^{-3}xF$

$$\text{Cutting cost[Euro/m]} = \frac{2.654 + 1.376 \times \text{P[kW]} + 9.60\ \text{x}10^{-3} \times \text{F[l/hr]}}{(0.85) \times \text{S[mm/min][60min/hr][m/1000mm]}} \quad (1)$$

$$\text{cutting cost[Euro/m]} = \frac{2.654 + 1.376 \times \text{P} + 9.60\text{x}10^{-3} \times \text{F}}{0.051 \times \text{S}} \quad (2)$$

Where

P: used out put power in kW.
F: flow rate in l/hr.
S: cutting speed in mm/min.

The compressed nitrogen will flow in a supersonic manner within the pressure range used in this work. Consequently, the flow rate in [l/hr] of this fluid through a nozzle can be easily calculated from Eq. 3 [1].

$$\text{Flow Rate}\,[\text{l/hr}] = \text{F} = 492 \times d^{2}\left(p_{g} + 1\right) \qquad (3)$$

Where:

d: Nozzle diameter [mm].

P_g: Nozzle supply pressure [bar].

4. Results and Discussion

4.1 Analysis of Variance

Design expert software V7 was used to analyze the measured responses. The fit summary output indicates that for all responses, the quadratic models are statistically recommended for further analysis as they have the maximum predicted and adjusted R^2 [23 and 24]. The test for significance of the regression models, the test for significance on individual model coefficients and the lack of fit test were performed using the same statistical package for all responses. By selecting the step-wise regression method, the insignificant model terms can be automatically eliminated. The resulting ANOVA tables (Tables 5 to 9) for the reduced quadratic models outline the analysis of variance for each response and illustrate the significant model terms. The same tables show also the other adequacy measures R^2, Adjusted R^2 and Predicted R^2.

The entire adequacy measures are close to 1 which are in reasonable agreement and indicates adequate models [16, 17 and 24]. The adequate precision compares the range of the predicted value at the design points to the average prediction error. In all cases the values of adequate precision ratios are dramatically greater than 4. An adequate precision ratio above 4 indicates that the model is adequate [23 and 25]. An adequate model means that the reduced model has successfully passed all the required statistical tests and can be used to predict the responses or to optimize the process etc.

For the upper kerf model the analysis of variance indicates that the main effect of all the following factors, quadratic effect of laser power (A^2), cutting speed (B^2), focal position (C^2) and nitrogen pressure (D^2) are the most significant model terms associated with this response. However, the interaction effect between cutting speed and nitrogen pressure (BC) is also affecting this response. While, for the lower kerf model, the analysis indicates that the main

effect of all factors, the quadratic effect of (A^2), (B^2), (C^2) and the interaction effect between (AE), (BD), (BE), (CD) and (DE) are the significant model terms. The analysis demonstrates that the cutting speed has the main role on the lower kerf width, then the laser power. For the ratio model, the analysis demonstrates that, the main effect of all the following factors, the quadratic effect of (A^2), (B^2), (C^2), (D^2) and the interaction effect between (BD) and (CD) are the significant model terms. All the findings for kerf width are in agreement with the results reported in [4, 7, 8 and 9]. Then, for the roughness model, it is evident from the analysis that the main effect of the laser power (A), cutting speed (B), focal point position (C), nitrogen pressure (D), the quadratic effects of cutting speed (B^2), focal position (C^2) and nitrogen pressure (D^2) are the significant terms. However, cutting speed is the factor which has the most significant effect on the roughness a funding which agrees with [11]. The focal position and laser power also affect the roughness notably. All the above findings are in agreement with the results found in [11]. Finally, for the operating cost model the results demonstrate that the main effect of laser power (A), cutting speed (B), nitrogen pressure (D), nozzle diameter (E), the interaction effects of laser power with nitrogen pressure (AD), laser power with nozzle diameter (AE), nitrogen pressure with nozzle diameter (DE), the quadratic effect of cutting speed (B^2) and nitrogen pressure (D^2) are the significant model terms related to operating cost. The final mathematical models in terms of actual factors as determined by design expert software are shown in Eqs 4-18:

Table 5: ANOVA table for upper kerf width reduced quadratic model.

Source	Sum of Squares	DF	Mean Square	F Value	Prob > F	
Model	0.0741	11	0.0067	31.060	< 0.0001	Significant
A	0.0057	1	0.0057	26.297	< 0.0001	
B	0.0353	1	0.0353	162.761	< 0.0001	
C	0.0083	1	0.0083	38.202	< 0.0001	
D	0.0100	1	0.0100	46.132	< 0.0001	
E	0.0076	2	0.0038	17.493	< 0.0001	
BC	0.0008	1	0.0008	3.835	0.0584	
A^2	0.0050	1	0.0050	23.150	< 0.0001	
B^2	0.0011	1	0.0011	5.203	0.0289	
C^2	0.0048	1	0.0048	22.195	< 0.0001	
D^2	0.0047	1	0.0047	21.465	< 0.0001	
Residual	0.0074	34	0.0002			
Lack of Fit	0.0066	29	0.0002	1.469	0.3583	Not Sig.
Pure Error	0.0008	5	0.0002			
Cor Total	0.0814	45				
$R^2 = 0.910$			Pred $R^2 = 0.839$			
Adj $R^2 = 0.880$			Adeq Precision = 20.808			

Table 6: ANOVA table for lower kerf width reduced quadratic model.

Source	Sum of Squares	DF	Mean Square	F Value	Prob > F	
Model	0.0323	17	0.0019	9.711	< 0.0001	Significant
A	0.0032	1	0.0032	16.378	0.0004	
B	0.0111	1	0.0111	56.578	< 0.0001	
C	0.0006	1	0.0006	3.197	0.0846	
D	0.0006	1	0.0006	3.050	0.0917	
E	0.0003	2	0.0001	0.726	0.4929	
AE	0.0011	2	0.0006	2.872	0.0733	
BD	0.0016	1	0.0016	8.322	0.0075	
BE	0.0010	2	0.0005	2.683	0.0859	
CD	0.0026	1	0.0026	13.046	0.0012	
DE	0.0015	2	0.0008	3.926	0.0314	
A^2	0.0008	1	0.0008	3.951	0.0567	
B^2	0.0020	1	0.0020	10.486	0.0031	
C^2	0.0079	1	0.0079	40.47176	< 0.0001	
Residual	0.0055	28	0.000195			
Lack of Fit	0.004871	23	0.000212	1.758863	0.2768	Not Sig.
Pure Error	0.000602	5	0.00012			
Cor Total	0.037744	45				
$R^2 = 0.855$			Pred $R^2 = 0.542$			
Adj $R^2 = 0.767$			Adeq Precision = 12.065			

Table 7: ANOVA table for ratio reduced quadratic model.

Source	Sum of Squares	DF	Mean Square	F Value	Prob > F	
Model	1.9997	12	0.1666	9.091	< 0.0001	Significant
A	0.0000	1	0.0000	0.000	0.9861	
B	0.0560	1	0.0560	3.057	0.0897	
C	0.3178	1	0.3178	17.339	0.0002	
D	0.1387	1	0.1387	7.568	0.0096	
E	0.2862	2	0.1431	7.806	0.0017	
BD	0.1507	1	0.1507	8.223	0.0072	
CD	0.1547	1	0.1547	8.442	0.0065	
A^2	0.3558	1	0.3558	19.408	0.0001	
B^2	0.2954	1	0.2954	16.118	0.0003	
C^2	0.9395	1	0.9395	51.256	< 0.0001	
D^2	0.1395	1	0.1395	7.610	0.0094	
Residual	0.6049	33	0.0183			
Lack of Fit	0.5138	28	0.0184	1.007827	0.5597	Not Sig.
Pure Error	0.0910	5	0.018209			
Cor Total	2.604571	45				
$R^2 = 0.855$			Pred $R^2 = 0.511$			
Adj $R^2 = 0.683$			Adeq Precision = 12.300			

Table 8: ANOVA table for roughness reduced quadratic model.

Source	Sum of Squares	DF	Mean Square	F Value	Prob > F	
Model	4.1410	7	0.5916	17.8507	< 0.0001	Significant
A	0.2806	1	0.2806	8.4681	0.0060	
B	1.2778	1	1.2778	38.5585	< 0.0001	
C	0.9195	1	0.9195	27.7462	< 0.0001	
D	0.0735	1	0.0735	2.2188	0.1446	
B^2	1.5248	1	1.5248	46.0097	< 0.0001	
C^2	0.1089	1	0.1089	3.2856	0.0778	
D^2	0.2081	1	0.2081	6.2789	0.0166	
Residual	1.2593	38	0.0331			
Lack of Fit	1.2331	33	0.0374	7.1325	0.0184	Not Sig. at α=0.01
Pure Error	0.0262	5	0.0052			
Cor Total	5.4004	45				
$R^2 = 0.767$			Pred $R^2 = 0.635$			
Adj $R^2 = 0.734$			Adeq Precision = 16.956			

Table 9: ANOVA table for operating cost reduced quadratic model.

Source	Sum of Squares	DF	Mean Square	F Value	Prob > F	
Model	12.884206	12	1.0737	15774705.83	< 0.0001	Significant
A	0.000105	1	0.0001	1542.23	< 0.0001	
B	4.827796	1	4.8278	70930617.16	< 0.0001	
D	0.525086	1	0.5251	7714639.87	< 0.0001	
E	7.256601	2	3.6283	53307470.27	< 0.0001	
AD	0.000001	1	0.0000	10.97	0.0022	
AE	0.000016	2	0.0000	117.16	< 0.0001	
DE	0.000095	2	0.0000	698.08	< 0.0001	
B^2	0.204422	1	0.2044	3003398.42	< 0.0001	
D^2	0.002628	1	0.0026	38618.03	< 0.0001	
Residual	0.000002	33	6.81E-08			
Cor Total	12.884209	45				
$R^2 = 0.855$			Pred $R^2 = 0.511$			
Adj $R^2 = 0.683$			Adeq Precision = 12.300			

The mathematical models for nozzle diameter of 1 mm are as follows:

$$\begin{aligned}\text{Upper Kerf} = {} & -1.27254 + 1.03467 * \text{Laser power} - 4.47361E\text{-}005 * \text{Cutting speed} \\ & -0.13479 * \text{Focal position} + 0.10236 * \text{Nitrogen pressure} \\ & -1.44167E\text{-}005 * \text{Cutting speed} * \text{Focal position} - 0.38367 * \text{Laser power}^2 \\ & -1.13681E\text{-}008 * \text{Cutting speed}^2 - 0.023479 * \text{Focal position}^2 \\ & -3.69444E\text{-}003 * \text{Nitrogen pressure}^2 \end{aligned} \quad (4)$$

Lower Kerf = 0.81013 - 0.33202 * Laser power - 2.14646E-006 * Cutting speed
+ 0.30630 * Focal position -1.76667E-003 * Nitrogen pressure
-8.06667E-006 * Cutting speed * Nitrogen pressure
-0.010100 * Focal position * Nitrogen pressure
+0.14481 * Laser power^2 + 1.47449E-008 * Cutting speed^2
+0.028967 * Focal position^2 (5)

Ratio = -12.12985 +8.07832 * Laser power - 2.93788E-004 * Cutting speed
-3.09299 * Focal position + 0.62368 * Nitrogen pressure
+7.76458E-005 * Cutting speed * Nitrogen pressure
+0.078674 * Focal position * Nitrogen pressure
-3.23038 * Laser power^2 -1.83990E-007 * Cutting speed^2
-0.32810 * Focal position^2 - 0.020228 * Nitrogen pressure^2 (6)

Ra = 6.52117 - 0.52975 * Laser power -1.28860E-003 * Cutting speed
+0.39008 * Focal position - 0.60755 * Nitrogen pressure
+3.92802E-007 * Cutting speed^2 + 0.10497 * Focal position^2
+0.023217 * Nitrogen pressure^2 (7)

Ln(Operating cost) = -0.048359 + 0.028837 * Laser power - 1.12461E-003*
Cutting speed + 0.13613 * Nitrogen pressure –
6.91362E-004* Laser power * Nitrogen pressure +
1.43825E-007 * Cutting speed^2 - 2.60941E-003 *
Nitrogen pressure^2 (8)

The mathematical models for nozzle diameter of 1.5 mm are as follows:

Upper Kerf = -1.23634+ 1.03467 * Laser power - 4.47361E-005 * Cutting speed
-0.13479 * Focal position + 0.10236 * Nitrogen pressure
-1.44167E-005 * Cutting speed * Focal position - 0.38367 *
` Laser power^2-1.13681E-008 * Cutting speed^2 - 0.023479 *
Focal position^2 -3.69444E-003 * Nitrogen pressure^2 (9)

Lower Kerf = 0.86483- 0.28769* Laser power +1.61035E-005* Cutting speed
+ 0.30630 * Focal position -0.013622* Nitrogen pressure
-8.06667E-006 * Cutting speed * Nitrogen pressure
-0.010100 * Focal position * Nitrogen pressure
+0.14481 * Laser power^2 + 1.47449E-008 * Cutting speed^2
+0.028967 * Focal position^2 (10)

$$\text{Ratio} = -11.9074 + 8.07832 * \text{Laser power} - 2.93788E\text{-}004 * \text{Cutting speed} - 3.09299 * \text{Focal position} + 0.62368 * \text{Nitrogen pressure} + 7.76458E\text{-}005 * \text{Cutting speed} * \text{Nitrogen pressure} + 0.078674 * \text{Focal position} * \text{Nitrogen pressure} - 3.23038 * \text{Laser power}^2 - 1.83990E\text{-}007 * \text{Cutting speed}^2 - 0.32810 * \text{Focal position}^2 - 0.020228 * \text{Nitrogen pressure}^2 \quad (11)$$

$$\text{Ra} = 6.52117 - 0.52975 * \text{Laser power} - 1.28860E\text{-}003 * \text{Cutting speed} + 0.39008 * \text{Focal position} - 0.60755 * \text{Nitrogen pressure} + 3.92802E\text{-}007 * \text{Cutting speed}^2 + 0.10497 * \text{Focal position}^2 + 0.023217 * \text{Nitrogen pressure}^2 \quad (12)$$

$$\text{Ln(Operating cost)} = +0.70636 + 0.018053 * \text{Laser power} - 1.12461E\text{-}003 * \text{Cutting speed} + 0.13877 * \text{Nitrogen pressure} - 6.91362E\text{-}004 * \text{Laser power} * \text{Nitrogen pressure} + 1.43825E\text{-}007 * \text{Cutting speed}^2 - 2.60941E\text{-}003 * \text{Nitrogen pressure}^2 \quad (13)$$

The mathematical models for nozzle diameter of 2 mm are as follows:

$$\text{Upper Kerf} = -1.24154 + 1.03467 * \text{Laser power} - 4.47361E\text{-}005 * \text{Cutting speed} - 0.13479 * \text{Focal position} + 0.10236 * \text{Nitrogen pressure} - 1.44167E\text{-}005 * \text{Cutting speed} * \text{Focal position} - 0.38367 * \text{Laser power}^2 - 1.13681E\text{-}008 * \text{Cutting speed}^2 - 0.023479 * \text{Focal position}^2 - 3.69444E\text{-}003 * \text{Nitrogen pressure}^2 \quad (14)$$

$$\text{Lower Kerf} = 0.92446 - 0.38535 * \text{Laser power} - 3.00202E\text{-}005 * \text{Cutting speed} + 0.30630 * \text{Focal position} - 0.010300 * \text{Nitrogen pressure} - 8.06667E\text{-}006 * \text{Cutting speed} * \text{Nitrogen pressure} - 0.010100 * \text{Focal position} * \text{Nitrogen pressure} + 0.14481 * \text{Laser power}^2 + 1.47449E\text{-}008 * \text{Cutting speed}^2 + 0.028967 * \text{Focal position}^2 \quad (15)$$

$$\text{Ratio} = -12.0057 + 8.07832 * \text{Laser power} - 2.93788E\text{-}004 * \text{Cutting speed} - 3.09299 * \text{Focal position} + 0.62368 * \text{Nitrogen pressure} + 7.76458E\text{-}005 * \text{Cutting speed} * \text{Nitrogen pressure} + 0.078674 * \text{Focal position} * \text{Nitrogen pressure} - 3.23038 * \text{Laser power}^2 - 1.83990E\text{-}007 * \text{Cutting speed}^2 - 0.32810 * \text{Focal position}^2 - 0.020228 * \text{Nitrogen pressure}^2 \quad (16)$$

$$Ra = 6.52117 - 0.52975 * \text{Laser power} - 1.28860E\text{-}003 * \text{Cutting speed} + 0.39008 * \text{Focal position} - 0.60755 * \text{Nitrogen pressure} + 3.92802E\text{-}007 * \text{Cutting speed}^2 + 0.10497 * \text{Focal position}^2 + 0.023217 * \text{Nitrogen pressure}^2 \quad (17)$$

$$\ln(\text{Operating cost}) = +1.26155 + 0.013946 * \text{Laser power} - 1.12461E\text{-}003 * \text{Cutting speed} + 0.13975 * \text{Nitrogen pressure} - 6.91362E\text{-}004 * \text{Laser power} * \text{Nitrogen pressure} + 1.43825E\text{-}007 * \text{Cutting speed}^2 - 2.60941E\text{-}003 * \text{Nitrogen pressure}^2 \quad (18)$$

4.2 Validation of the models.

To confirm the adequacy of the developed models, three confirmation experiments were carried out using new randomly selected test conditions, each within the experiment range defined earlier in chapter 4. Using the point prediction option in the software, the values of all responses of the validation experiments were predicted using the previous developed models and compared with the experimentally measured responses values for these confirmation experiments. Table 10 summarizes the experimental conditions, actual experimental values, predicted values and percentage error in prediction. It is evident that the models can adequately describe the responses within the ranges considered as the maximum error percent in prediction is 9.292% which is in good agreement. All the percentage errors are in agreement with the values reported in [16 and 17].

Table 10: Confirmation experiments for AISI 316L.

Exp. No.	A	B	C	D	E		Upper kerf	Lower kerf	ratio	R_a	Cost
1	1	3000	-3	12.5	1	Actual	0.159	0.138	1.152	1.582	0.4431
						Predicted	0.167	0.145	1.104	1.469	0.4432
						Error %	-5.036	-5.179	4.210	7.164	-0.0247
2	1.5	1000	-3	12.5	1	Actual	0.286	0.237	1.207	0.704	1.3428
						Predicted	0.299	0.248	1.223	0.639	1.3431
						Error %	-4.431	-4.703	-1.364	9.292	-0.024
3	1.5	1000	-3	15	2	Actual	0.317	0.261	1.215	0.773	6.0197
						Predicted	0.332	0.238	1.120	0.716	6.0207
						Error %	-4.600	8.884	7.788	7.387	-0.016

4.3 Effect of process parameters on the responses

4.3.1 Upper kerf

The perturbation plot for the upper kerf width is shown in Fig. 1. The perturbation plot helps to compare the effect of all factors at a particular point in the design space. This type of display does not show the effect of interactions. The lines represent the behaviours of each factor, while holding the others constant (i.e. centre point by default). In the case of more than one factor this type of display could be used to find those factors that most affect the response. It is evident from Fig. 1 that the upper kerf width increases as the laser power and gas pressure increase, which agrees with [6, 7 and 8], yet above the centre values of both factors the upper kerf becomes stable. However, the upper kerf width sharply decreases as the cutting speed increases. This is in a good agreement with [7 and 8]. In the case of the focal point position, it is notable that as the focal position increases up to the centre point (C = -3 mm) the upper kerf slightly increases, but, as the focal point increases beyond this point the upper kerf begins to decrease.

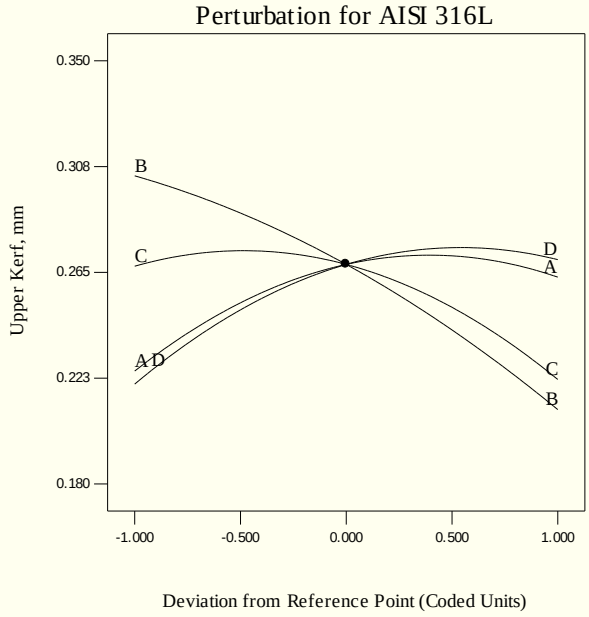

Fig. 1: Perturbation plot showing the effect of process parameters on upper kerf width.

Table 11 presents the overall percentage change in the upper kerf width as a result of changing each factor from its lowest value to its highest value while keeping the other factor at their centre values. It is evident from Table 11 that the cutting speed is the main factor influencing the upper kerf width, this result agrees with the results found in [7 and 8]. Fig. 2 is a

contour graph demonstrating the effect of both laser power and cutting speed on the upper kerf width at two nozzle diameters 1 and 1.5 mm. In fact, all the investigated LBC parameters are found to affect the upper kerf, and this outcome agrees with [4].

Table 11: Percentage change in upper kerf as each factor increases.

Factor	Percentage change in upper kerf, %
Laser power	Increases by 16.75
Cutting speed	Decreases by 30.92
Focal position	Decreases by 17.01
Nitrogen pressure	Increases by 22.72
Nozzle diameter	Increases by 11.56

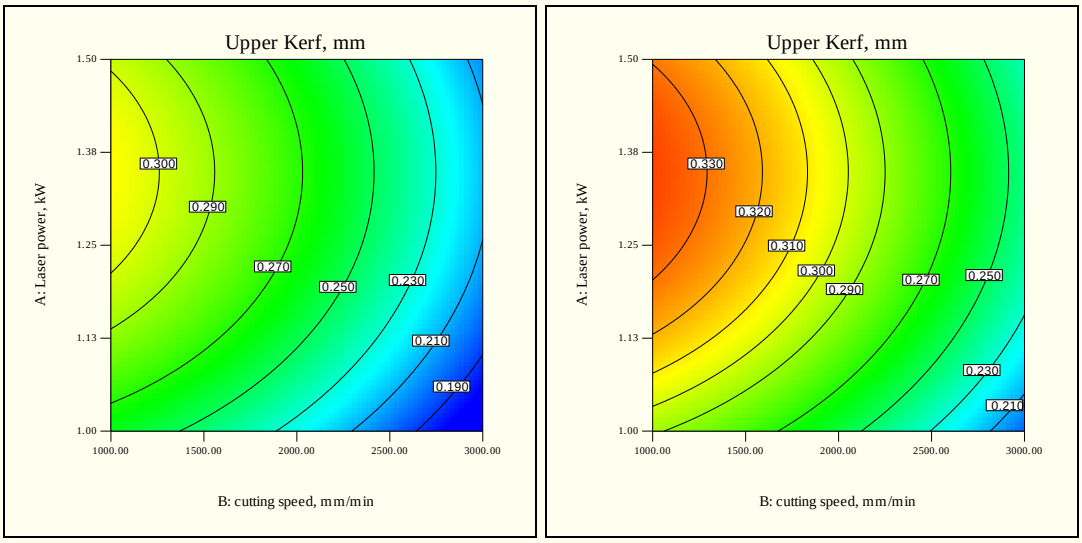

(a) (b)

Fig. 2: Contours plot showing the effect of laser power and cutting speed on the upper kerf width at different nozzle diameters (a) 1 mm and (b) 1.5 mm.

4.3.2 Lower kerf

It is clear from Fig. 3 that the lower kerf width increases as the laser power and the gas pressure increase. However, this response decreases with the increase in the focal point position up to the midpoint (i.e. -3 mm) and then starts to increase as the focal point position increases from -3 mm towards -2 mm. This incident could be related to the interaction between the gas

pressure and the focal point position, which will be discussed later. Also, the lower kerf decreases as the cutting speed increases this is in agreement with findings reported in [8].

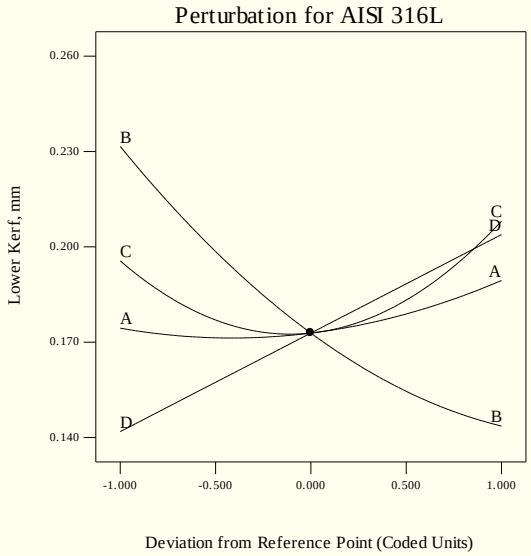

Fig. 3: Perturbation plot showing the effect of process parameters on lower kerf width.

The interaction plots help the researchers to find the best parameter settings that lead to the smaller possible lower kerf or the desirable response value. Fig. 4 demonstrates the interaction effect between the cutting speed and nitrogen pressure on the lower kerf width. It is clear that at low cutting speeds below 2100 mm/min a smaller lower kerf width of 0.170 mm could be obtained if the lowest nitrogen pressure of 10 bar is used. On the other hand, at higher cutting speeds above 2100 mm/min the smallest lower kerf width of 0.14 mm could be produced if the highest nitrogen pressure of 15 bar was supplied. At cutting speeds of about 2100 mm/min both levels of nitrogen pressure have the same effect on the lower kerf width. Fig. 5 shows the interaction effect between the focal point position and the nitrogen pressure. It is evident that the use of a wider laser beam (i.e. focal position of - 4 mm) leads a small lower kerf width of 0.17 only if the lowest gas pressure of 10 bar is applied. On the other hand, using a narrower laser beam (i.e. focal position of - 2 mm) results in a small lower kerf width only when the highest nitrogen pressure of 15 bar was applied. However, the nitrogen pressure would have the same effect on the lower kerf width if a focal point position just above -3 mm was employed. Dilthey et al. [9] have reported that exact adjustment of focal position and gas jet is essential, which supports the above findings. It is clear from the interaction graph shown in Fig. 6 that when using

a nozzle diameter of 1.5 mm there is no significant difference between the lower kerf width values produced by supplying either level of nitrogen pressures. This supports the idea of fixing the nozzle diameter to 1.5 mm in the optimization for the first criterion. It is evident from Table 12 that the nitrogen pressure and cutting speed are the main factors influencing the lower kerf width.

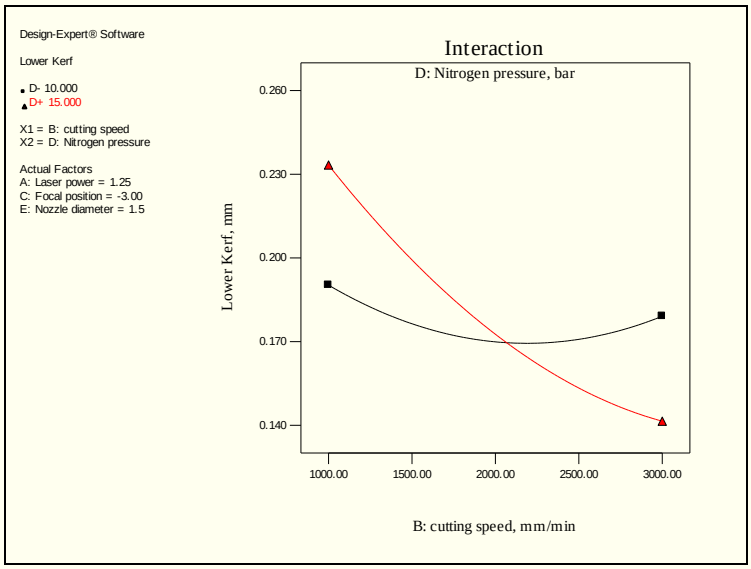

Fig. 4: Interaction plot showing the interaction between the cutting speed and the nitrogen pressure on the lower kerf.

Table 12: Percentage change in lower kerf as each factor increases.

Factor	Percentage change in lower kerf, %
Laser power	Increases by 8.60
Cutting speed	Decreases by 38.00
Focal position	Increases by 6.39
Nitrogen pressure	Increases by 43.71
Nozzle diameter	Increases by 3.09

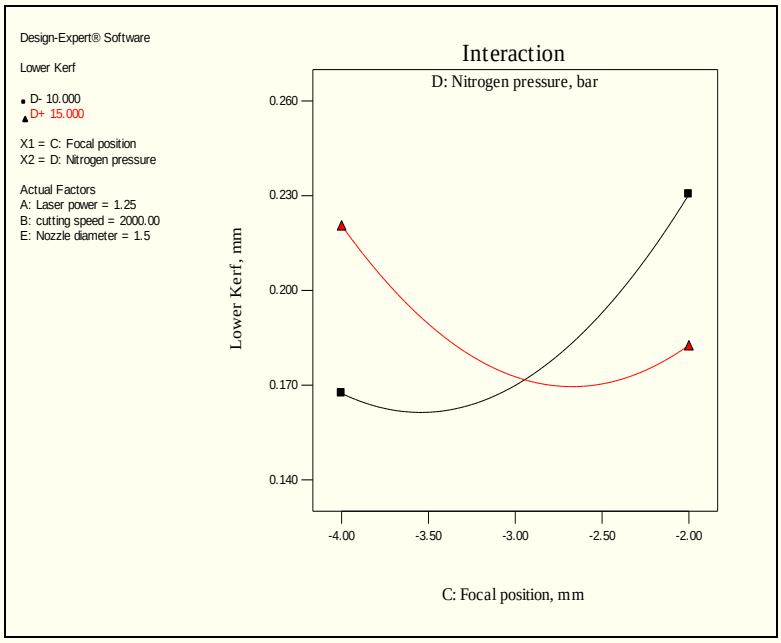

Fig. 5: Interaction plot showing the interaction between the focal position and the nitrogen pressure on the lower kerf.

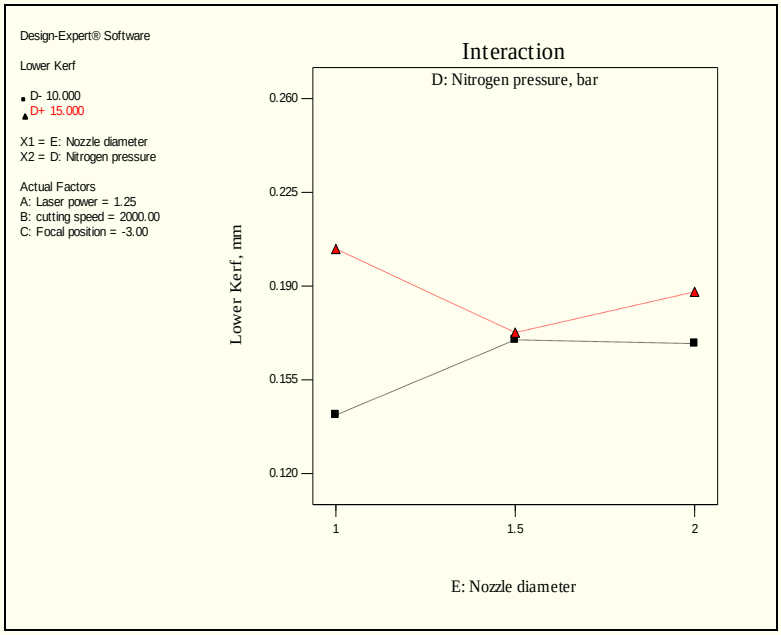

Fig. 6: Interaction plot showing the interaction between the nozzle diameter and the nitrogen pressure on the lower kerf.

4.3.3 Ratio

Fig. 7 is an interaction plot showing the influence of cutting speed and nitrogen pressure on the ratio. It is apparent that by using cutting speeds below 1520 mm/min the ratio would be less (close to one) if the highest nitrogen pressure of 15 bar was supplied. Above this value of cutting speed the ratio would be less if the lowest nitrogen pressure of 10 bar was used. The same trend was noticed as the nozzle diameter changed. From the interaction graph shown in Fig. 8 it is obvious that by using focal position below -3.48 mm the ratio would be close to one if the highest nitrogen pressure of 15 bar was used. Above -3.48 the ratio would be close to one as the lowest nitrogen pressure of 10 bar was used. It is evident from Table 13 that the focal position and nitrogen pressure are the main factors influencing the ratio. These findings are in fair agreement with results reported in [10]. The results show that the range of the ratio lays between 0.94 and 1.93 for AISI316L. Therefore, a target ratio of one in this case will be a desirable goal when searching for the optimal condition to obtain a square cut edge.

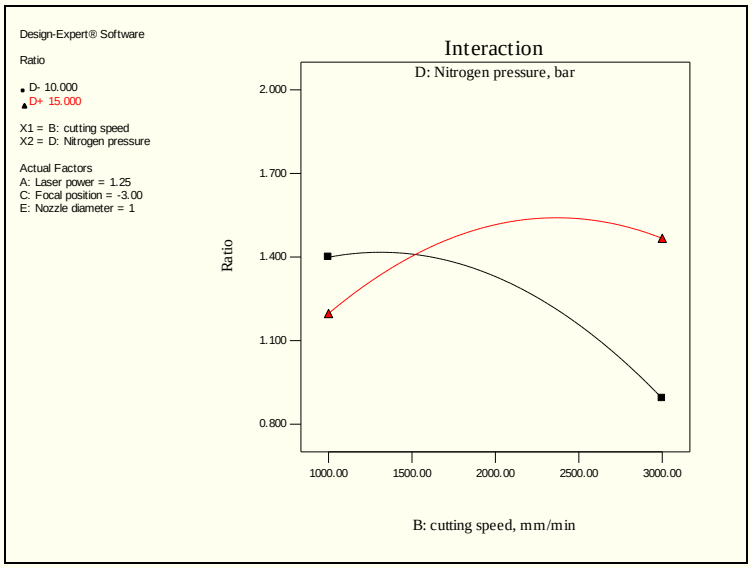

Fig. 7: Interaction plot showing the interaction between the cutting speed and the nitrogen pressure on the ratio.

Table 13: Percentage change in ratio as each factor increases.

Factor	Percentage change in ratio, %
Laser power	Increases by 0.09
Cutting speed	Decreases by 8.31
Focal position	Decreases by 20.69
Nitrogen pressure	Increases by 14.00
Nozzle diameter	Increases by 8.02

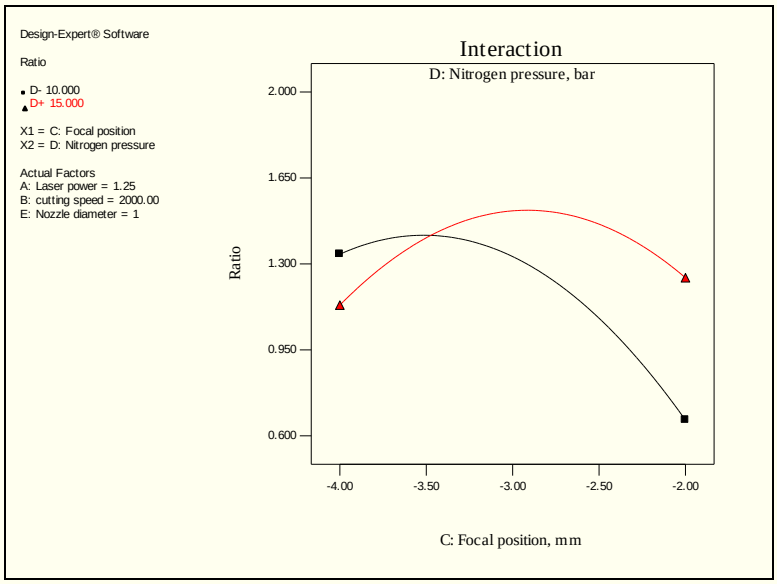

Fig. 8: Interaction plot showing the interaction between the focal position and the nitrogen pressure on the ratio.

4.3.4 Surface roughness

Fig. 9 is a perturbation plot showing the effect of all laser cutting parameters on the roughness of the cut surface. It is evident from the results that the R_a value decreases as the laser power, focal point position and nitrogen pressure increase; these finding are in agreement with [11] and disagree with [12]. However, the R_a value starts to rise as the nitrogen pressure increases above 13.4 bar as can be seen in Fig. 9. Moreover, the roughness decreases slightly as the cutting speed increases up to 1505 mm/min, which agrees with [12]. Between 1505 – 1740 mm/min the surface roughness values become stable, and then they remarkably increase as the cutting speed increases above 1740 mm/min, which disagrees with [12]. The results confirm that the nozzle diameter has no significant effect on the roughness of the cut surface in contrast to the apparent

results in Fig. 9. It is clear from Table 14 that the cutting speed, focal position and laser power are the main factors influencing the cut surface roughness.

Table 14: Percentage change in roughness as each factor increases.

Factor	Percentage change in R_a, %
Laser power	Decreases by 33.39
Cutting speed	Increases by 73.31
Focal position	Decreases by 47.68
Nitrogen pressure	Decreases by 15.52
Nozzle diameter	No effect

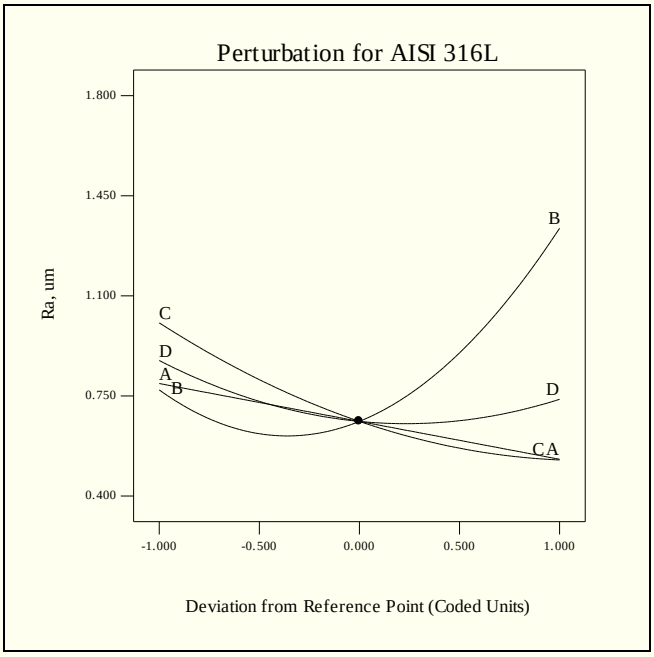

Fig. 9: Perturbation plot showing the effect of process parameters on roughness.

4.3.5 Operating cost

The perturbation plot would help to compare the effect of all the factors at a particular point in the design space. It is evident from Fig.10, that in the case of cutting speed, steep curvatures indicate that the responses are too sensitive to this factor. Also, Fig. 10a-c demonstrates the importance of the nozzle diameter with respect to the operating cost, while the steep slopes in the case of laser power and nitrogen pressure indicate that the operating cost is

less sensitive to these factors. In addition, the results indicate that as the laser power, nitrogen pressure and nozzle diameter increase the operating cost increases too. On the other hand, as the cutting speed increases the operating cost decreases sharply. These results are intuitive because more electrical power will be consumed as the laser power increases. Also, more gas will be consumed as both the nitrogen pressure and the nozzle diameter increase. However, the cost will decrease as the cutting speed increases due to the fact that the cutting will be performed in less time, and consequently, less electrical power and nitrogen gas will be consumed. Fig. 10 is a perturbation plot illustrating the above findings. It is apparent that the nozzle diameter, cutting speed and nitrogen pressure are the key factors affecting the operating cost. Moreover, these changes in the operating cost in terms of percentages are presented in Table 15 as each factor increases from its lowest level to its highest level. It is clear that the focal position has no effect on the operating cost.

On balance, it is evident from the above results for AISI316L that all the process parameters considered in this research affect the quality features somehow. Furthermore, in some cases, these parameter may interact in such a way that it becomes too hard to find the best cutting conditions which lead to the desired quality features. Therefore, an overall optimization should be performed for this material which would account for the minimization of the surface roughness, kerf widths and operating cost etc, or the maximization of the cut edge squareness. It is notable that the main factors affecting the operating cost are: nozzle diameter, cutting speed and minor effect of laser power

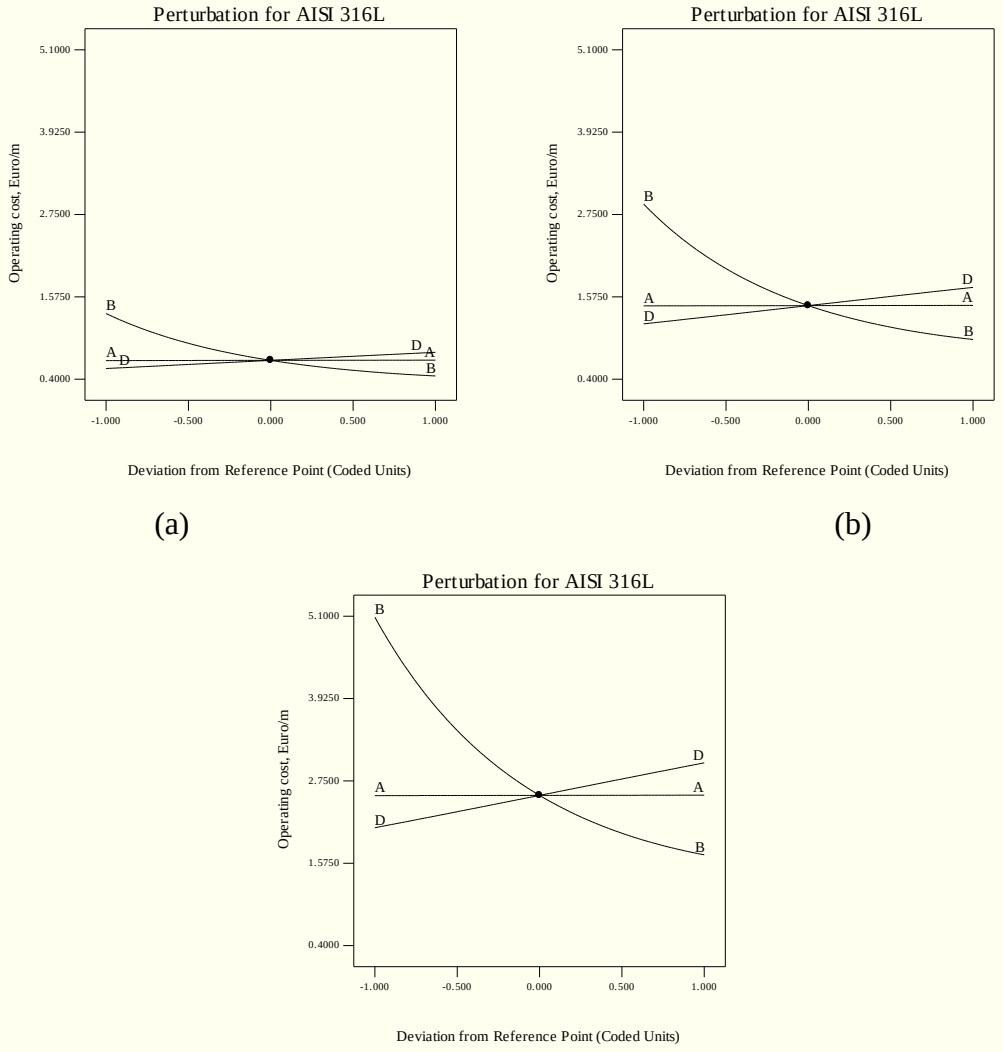

(a) (b)

(c)

Fig. 10: Perturbation plot illustrating the effect of process factors on operating cost at different nozzle diameters (a) 1 mm, (b) 1.5 mm and (c) 2 mm.

Table 15: Percentage change in cost as each factor increases.

Factor	Percentage change in cost, %
Laser power	Increases by 1.01
Cutting speed	Decreases by 66.67
Focal position	No effect
Nitrogen pressure	Increases by 41.92
Nozzle diameter	Increases by 280.59

5. OPTIMIZATION

Laser cutting is a multi-input and multi-output process that needs to be assessed carefully in order to achieve the most desirable results. Planning the fabrication of parts based on quality of the final cut surface alone may have important cost implications, which should be evaluated. Based on the previously presented results and discussion it is clear that there are many factors and their interactions, which affect the process. Thus, an in-depth optimization is required. To run any optimization it is important to know the following: the effect of each factor and its interaction effect with the other factors on the responses, the output of the process (i.e. responses) and finally the desirable criterion (i.e. the goal). In the numerical optimization for this research two criteria were used. The difference between these two criteria is that in the first criterion there were no restrictions on the process input parameters and the output quality features were set to achieve the highest quality in terms of surface roughness and cut edge perpendicularity (referring to this criterion as Quality). In the second criterion, the cost of the cutting is the main issue; consequently, some restrictions have been put on the process input parameters which have an effect on the operating cost. Also, regarding the second criterion, the operating cost was set to be a minimum with no restrictions on the other responses (referring to this criterion as Cost). This multi-responses optimization is solved via the desirability approach explained earlier in chapter 3, which is built in the Design expert software. Two types of optimization layout are available in Design expert. The first one, the numerical optimization feature, which finds a point or more in the factors domain that, would maximize the overall desirability (i.e. objective function). The second one, the graphical optimization, where the optimal range of each response has to be brought from the numerical optimization results in order to present them graphically. The graphical optimization allows visual selection of the optimal cutting conditions according to certain criterion. Graphical optimization results in plots called overlay plots. These plots are extremely practical for technical use at the workshop and help the operator to choose the optimal values of the laser cutting parameters to achieve the desirable response values for each material. The green/shaded areas on the overlay plots are the regions that meet the proposed criteria.

For this material the two optimization criteria are presented in Table 16. As seen in Table 16, that each factor and response have allocated a specific goal and importance. The nozzle

diameter was set at 1.5 mm. This value was chosen because it was found to be the best nozzle diameter that would lead to kerf widths close to each other, and consequently, a square cut edge.

5.1 Numerical optimization

Table 17 shows the optimal setting of the process parameters and the corresponding response values for both criteria for 2 mm AISI316L. It is noticeable that to obtain the superior quality cut with predicted ratio as close as possible to one and Ra ≈ 0.405 μm. The laser power has to be 1.49 kW with cutting speed between 1538-1661 mm/min, a focal point position of -2.02 mm, nitrogen pressure of around 11.4 bar and nozzle diameter of 1.5 mm have to be applied. Alternatively, if the reduction in the cutting cost is essential, it is confirmed that, a laser power of 1.02 kW has to be applied with cutting speed from 1900 to 2968 mm/min, a focal point position ranged from -3.92 mm to -2.85 mm, nitrogen pressure ranged between 10.4-12.9 bar and a nozzle diameter of 1 mm have to be used. It is clear that the roughness of cut section produced by using the setting of the first criterion is on average 65.8% smoother than the one produced by using the conditions of the second criterion. On the other hand, the cutting operating cost in the second criterion is on average 71% cheaper than that of the first criterion.

5.2 Graphical optimization

As mentioned earlier the range of each response has been chosen from the numerical optimization results in Table 17. These ranges were brought into the graphical optimization. Figures 11 and 12 show green areas which are the regions that comply with the first and second criteria respectively.

Table 16: Criteria for numerical optimization of AISI316L.

Factor or response	First criterion (Quality)		Second criterion (Cost)	
	Goal	Importance	Goal	Importance
Laser power	Is in range	3	Minimize	5
Cutting speed	Is in range	3	Maximize	5
Focal position	Is in range	3	Is in range	3
N_2 pressure	Is in range	3	Minimize	3
Nozzle Diameter	Equal to 1.5	3	Minimize	5
Upper Kerf	Is in range	3	Is in range	3
Lower Kerf	Is in range	3	Is in range	3
Ratio	Target to 1	5	Is in range	3
Roughness	Minimize	5	Is in range	3
Operating cost	Is in range	3	Minimize	5

Table 17: Optimal cutting conditions as obtained by Design-Expert for 2 mm thick AISI316L.

	No.	A, kW	B, mm/min	C, mm	D, bar	E, mm	Upper kerf, mm	Lower kerf, mm	Ratio	Ra, mm	Cost, €/m	Desirability
1st criterion Quality	1	1.49	1635	-2.02	11.3	1.5	0.26	0.251	1	0.409	1.66	1
	2	1.49	1636	-2.01	11.4	1.5	0.26	0.251	1	0.402	1.67	1
	3	1.49	1650	-2.01	11.4	1.5	0.26	0.251	1	0.401	1.66	1
	4	1.49	1661	-2.02	11.4	1.5	0.258	0.25	1	0.409	1.63	1
	5	1.49	1538	-2	11.4	1.5	0.265	0.254	1	0.409	1.78	1
2nd criterion Cost	1	1.02	2575	-3.32	11.7	1	0.198	0.145	1.243	1.195	0.48	0.8311
	2	1.22	2968	-3.92	11.4	1	0.208	0.146	1.099	1.685	0.41	0.7927
	3	1.03	2106	-3.11	11.1	1	0.21	0.151	1.31	0.919	0.57	0.7754
	4	1.02	2831	-3.08	12.9	1	0.19	0.15	1.246	1.303	0.48	0.7721
	5	1.04	1900	-2.85	10.4	1	0.198	0.154	1.199	0.878	0.60	0.7625

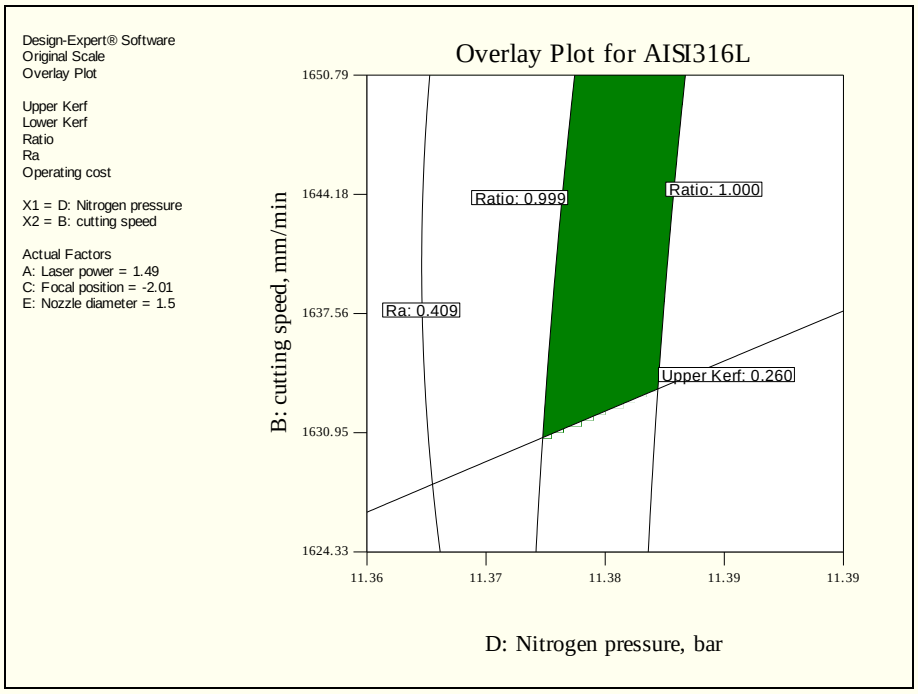

Fig. 11: Overlay plot shows the region of optimal cutting condition based on the first criterion for 2 mm AISI316L.

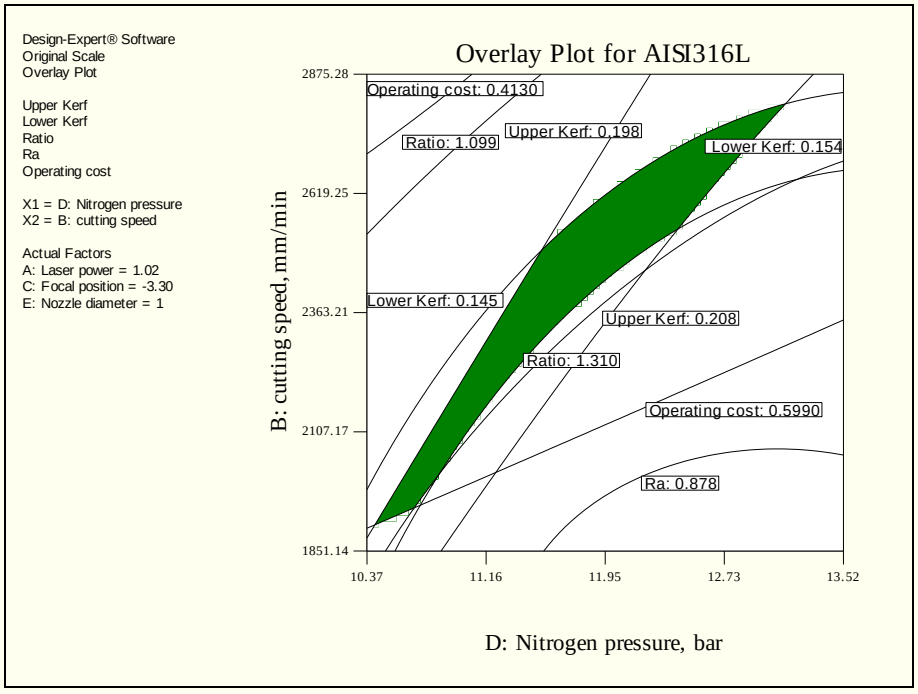

Fig. 12: Overlay plot shows the region of optimal cutting condition based on the second criterion for 2 mm AISI316L.

CONCLUSIONS

The following points can be concluded from this work within the factors limits:

1. The upper kerf width increases as the laser power, nitrogen pressure and nozzle diameter increase, and it decreases as the cutting speed and focal position increase. However, the cutting speed is the main factor affecting the upper kerf.
2. The laser power, nitrogen pressure and focal position have a positive effect on the lower kerf width. While, the cutting speed has a negative effect.
3. The ratio increases as the laser power, nitrogen pressure and nozzle diameter increase, and it decreases as the cutting speed and focal position increases.
4. The roughness value increases as the cutting speed increases and it decreases as the other parameters increases. However, the nozzle diameter has no significant effect on the roughness.
5. The optimal cutting setting for AISI316L are laser power of 1.49 kW, cutting speed between 1538 and 1661 mm/min, a focal point position of - 2.02 mm, nitrogen pressure of around 11.4 bar and nozzle diameter of 1.5 mm if the quality is important. The cut section roughness is on average 65.8% smoother if this setting was applied.
6. The economical optimal settings are laser power of 1.02 kW, cutting speed from 1900 to 2968 mm/min, a focal point position ranged from -3.92 mm to -2.85 mm, nitrogen pressure ranged between 10.4 and 12.9 bar and a nozzle diameter of 1 mm.
7. A reduction of about 71% in the cutting operating cost could be achieved, if the economical setting is considered.

Acknowledgments

The authors wish to thank Mr. Martin Johnson the laser expert in DCU and the School of Mechanical and Manufacturing Engineering, Dublin City University for the financial support of this work.

REFERENCE

[1] J. Powell, CO_2 Laser Cutting, 2nd Edition, Springer-Verlag Berlin Heidelberg, New York, (1998).

[2] W. M. Steen, Laser Material processing, Springer, London, 1991.

[3] S. L. Chen, The effects of gas composition on the CO_2 laser cutting of mild steel, J. Material Process Technology, Vol. 73, 1998, pp. 147–159.

[4] K. A. Ghany, M. Newishy, Cutting of 1.2mm thick austenitic stainless steel sheet using pulsed and CW Nd:YAG laser, J. of Materials Processing Technology, Vol. 168, 2005, pp. 438–447.

[5] S. L. Chen, The effects of high-pressure assistant-gas flow on high-power CO_2 laser cutting, J. Material Processing Technology, Vol. 88, 1999, pp. 57–66.

[6] I. Uslan, CO_2 laser cutting: kerf width variation during cutting, Proc. Of IMechE, Vol. 219 part B, J. of Engineering Manufacture, 2005, pp. 572-577.

[7] B. S. Yilbas, Effect of process parameters on the kerf width during the laser cutting process, Proc Instn Mech Engrs, Vol. 215 part B, J. of Engineering Manufacture, 2001, pp. 1357-1365.

[8] B. S. Yilbas, Laser cutting quality and thermal efficiency analysis, J. of Materials Processing Technology, Vol. 155-156, 2004, pp. 2106-2115.

[9] U. Dilthey, M. Faerber and J. Weick, Laser cutting of steel-cut quality depending on cutting parameters, J. of Welding in the World, Vol. 30, No. 9/10, 1992, pp. 275-278.

[10] B. S. Yilbas and M. Rashid, CO_2 laser cutting of Incoloy 800 HT alloy and its quality assessment, J. of Laser in Engineering, Vol. 12, No. 2, 2002, pp. 135-145.

[11] M. Radovanovic and P. Dasic, Research on surface roughness by laser cut, the Annals of University "Dunarea De Jos" of Galati Fascicle VII, ISSN 1221-4590, Tribology, 2006, pp. 84-88.

[12] R. Neimeyer, R. N. Smith and D. A. Kaminski, Effects of operating parameters on surface quality for laser cutting of mild steel, J. of Engineering for Industry, Vol. 115, 1993, pp. 359-362.

[13] A. K. Dubey and V. Yadava, Multi-objective optimization of laser beam cutting process, Optics and Laser Technology, Vol. 40, No. 3, (2008), pp. 562–570.

[14] A. K. Dubey and V. Yadava, Multi-objective optimization of Nd:YAG laser cutting of nickel-based superalloy sheet using orthogonal array with principal component analysis, Optics and Laser Engineering, Vol. 46, (2008), pp. 124–132.

[15] B. S. Yilbas, Laser cutting of thick sheet metals: Effects of cutting parameters on kerf size variations, J. of Materials Processing Technology, Vol. 201, No. 1-3, 26 May (2008), pp. 285-290.

[16] H. A. Eltawahni, A.G. Olabi, K. Y. Benyounis, Effect of process parameters and optimization of CO_2 laser cutting of ultra high-performance polyethylene, Materials & Design, Volume 31, Issue 8, September 2010, Pages 4029-4038**.**

[17] H. A. Eltawahni, A.G. Olabi, K. Y. Benyounis, Investigating the CO_2 laser cutting parameters of MDF wood composite material, Journal of optics and Laser Technology, Volume 43, Issue 3, April 2011, pp. 648-659.

[18] H. A. Eltawahni, A. G. Olabi, K. Y. Benyounis, Assessment and Optimization of CO_2 Laser Cutting Process of PMMA, AIP Conference Proceedings, v 1315, 1553-8, 2011; ISSN: 0094-243X; Conference: International Conference on Advances in Materials and Processing Technologies (AMPT 2010), 24-27 Oct. 2010, Paris, France; Publisher: American Institute of Physics, USA.

[19] I. A. Choudhury and S. Shirley, laser cutting of polymeric materials: An experimental investigation, journal of Optics and Laser Technology, Vol. 42, 2010, pp. 503-508.

[20] Chen-Hao Li, Ming-Jong Tsai, Ciann-Dong Yang, Study of optimal laser parameters for cutting QFN packages by Taguchi's matrix method, Optics & Laser Technology, Volume 39, Issue 4, June 2007, Pages 786-795.

[21] A. Sharma, V. Yadava, Modelling and optimization of cut quality during pulsed Nd:YAG laser cutting of thin Al-alloy sheet for straight profile, Optics & Laser Technology, In Press, Corrected Proof, Available online 20 July 2011.

[22] K. Y. Benyounis and A.G. Olabi, Optimization of different welding process using statistical and numerical approaches- A reference guide, Journal of Advances in Engineering Software, 39, (2008) 483-496.

[23] A. Ruggiero, L. Tricarico, A.G. Olabi, K. Y. Benyounis, Weld-bead profile and costs optimization of the CO_2 dissimilar laser welding process of low carbon steel

and austenitic steel AISI316, Optics & Laser Technology, Volume 43, Issue 1, February 2011, Pages 82-90.

[24] K. Y. Benyounis, A.G. Olabi and M. S. J. Hashmi, Multi-response optimization of CO_2 laser-welding process of austenitic stainless steel, Optics & Laser Technology, 40 (1) (2008) 76-87.

[25] A. G. Olabi, G. Casalion, K. Y. Benyounis, and M. S. J. Hashmi, Minimization of the residual stress in the heat affected zone by means of numerical methods, J. of Materials & Design, Vol. 28, No. 8, 2007, pp. 2295-2302.